A study of rotor topologies for line-start PM motors for cooling fan applications (repository copy)

Article:

Els, J. P., Sorgdrager, A. J., Wang, R.-J., (2014) A study of rotor topologies for line-start PM motors for cooling fan applications, *Proc. of the Southern African Universities Power Engineering Conference*, (SAUPEC), Durban, South Africa, pp. 284--289, 30-31 January 2014

A STUDY OF ROTOR TOPOLOGIES OF LINE-START PM MOTORS FOR COOLING FAN APPLICATIONS

Jéan-Pierre Els, Albert Sorgdrager and Rong-Jie Wang*

* *Department of Electrical and Electronic Engineering, Stellenbosch University, Private Bag X1, Matieland 7602, South Africa E-mail: rwang@sun.ac.za*

Abstract: The work presented in this paper deals with a study of different rotor topologies for line-start permanent magnet synchronous motors, which are compared and weighed up against each other to identify the best suited topology for fan type load applications. The design analysis and optimization of line-start permanent magnet machines are carried out by using a combination of finite element method and analytical models. The selected designs are optimized by formulating a cost function with key variables included. The optimization aims to optimize the permanent magnet weight with additional constraints to satisfy the required performance characteristics. The mass moment of inertia, the damping coefficient and the torque-speed curve of a practical cooling fan are experimentally determined, which are incorporated in the transient finite element analysis to evaluate the starting and synchronization capabilities of each candidate design. It is found that the rotor topology with asymmetrical magnet array delivers best overall performance.

Key words: Line-start motor; permanent magnet; induction motor; design optimization; finite element method; transient performance; cage winding.

1. INTRODUCTION

The energy consumption of the world is increasing at an alarming rate. Owing to the growing environmental concerns, the world increasingly focuses on energy saving programs [1]. Since electric motors are greatest energy consumption apparatuses, it is of critical importance to improve their energy efficiency. The induction motor (IM) constitutes, by far, the largest portion of electric motors both in terms of quantity and total power ratings among all electric motors [2].

Although significant amount of research and development effort has been dedicated to improve the performance of IMs, there is an inherent limit to their efficiency and power factor, especially at small power ratings. More efficient motor types gradually appear as alternatives. Amongst others, line-start permanent magnet synchronous machines (LSPMSMs) are increasingly receiving attention in recent years.

LSPMSMs have certain advantages over IMs such as higher efficiency and power factor within a wide load range. It is perceived that LSPMSMs could replace the IMs in many applications such as fans and pumps with better results. Due to the presence of a negative breaking torque generated by the permanent magnets (PM) during start-up, LSPMSMs are not suitable for all applications. The magnitude of this braking torque is influenced by the back-EMF voltage induced by the PM in the stator coils [3].

This paper investigates the feasibility of an LSPMSM to replace an IM for fan-type loads. Selected LSPMSM candidate designs with different rotor topologies are each optimally designed and compared to identify the best suited topology for fan-type load applications.

2. DESIGN SPECIFICATIONS

In this section the design specifications of a LSPMSM is described. For this study a WEG 2.2kW 525V 4-pole three-phase premium efficiency induction motor (PEIM) is selected as a reference motor. The stator design of the PEIM will be applied to all the LSPMSM designs so that only the rotors need to be optimally designed. From a production perspective, it would be cost-effective if standard IMs can be easily modified to LSPMSMs. The basic design specifications and dimensions are listed in Tables 1 and 2 respectively. The winding layout of the PEIM stator is given in Fig. 1.

Table 1: Design specifications.

Description	Value
Power, kW	2.2
Line voltage, V	525
Rated speed, RPM	1500
Number of phases	3
Number of poles	4
Duty cycle	S1
Frame size	100L

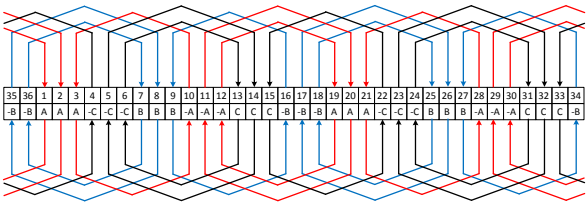

Figure 1: The winding layout of the induction motor stator.

Table 2: The dimensions of LSPMSM stator.

Description	Stator	Rotor
Outer diameter, mm	160	97.9
Inner diameter, mm	99.9	26.8
Stack length, mm	121	121
Wire diameter, mm	0.643	-
Winding type	lap	cage
Coil pitch	23/3	-
Phase connection	delta	-
Number of slots	36	28
Number of conductors per slot	82	-
Number of strands per conductor	2	-
Air-gap length, mm	0.5	-

2.1 *Characteristics of fan-type loads*

The load torque of a fan is proportional to the square of the fan rotation speed. This type of loads exhibit variable load torque characteristics. However most practical fans have to overcome a significant breakaway torque when starting [4]. Furthermore, the moment of inertia and damping coefficient of the load are also important factors. To start up a fan load, the transient torque profile of a LSPMSM should be designed in such a manner that the torque dip due to the PM breaking torque is higher than the required load torque. This is indicated in Fig. 2 with the black line representing the torque profile of the LSPMSM and the solid blue line the load torque profile of a fan-type load.

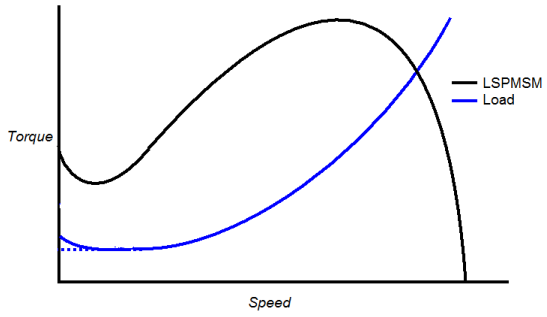

Figure 2: Torque-speed characteristics for fan-type load.

3. DESIGN AND OPTIMIZATION

This section presents the selected rotor topologies and the design optimization methodology and procedure of LSPMSMs.

3.1 *Selected rotor topologies*

The rotor topologies selected for the study are shown in Fig. 3. All four topologies are of embedded PMs as this allows more freedom of design with regards to the arrangements of PM arrays shapes [5]. In general, embedded LSPMSM rotor topologies have shown to provide better transient performance and stability over surface-mounted topologies but weaker steady-state performance [6]. Round rotor slots are selected for all the designs simply for ease of manufacturing at a later stage. The cage bar material is aluminium.

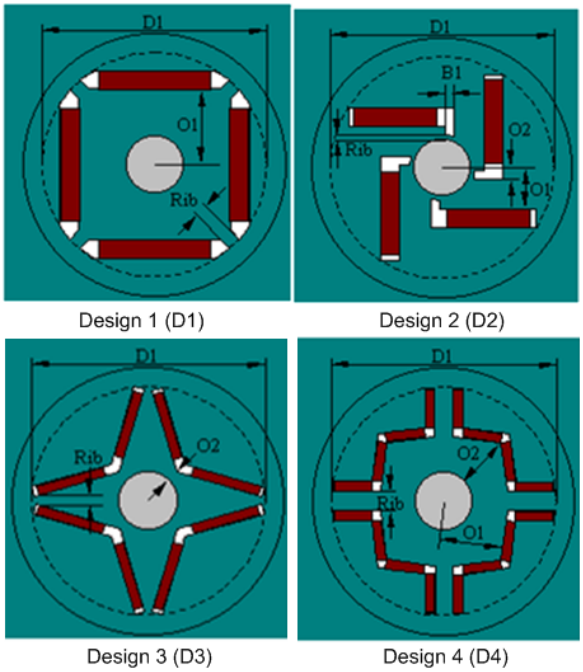

Figure 3: The selected LSPMSM rotor topologies showing key design variables.

3.2 *Optimization procedure*

The design of a LSPM motor is essentially a complicated multi-variable and multi-criteria optimization problem [7] as both steady-state and transient performance need to be taken into account. The basic design methodology employed here is to use a combination of both analytical and FEM performance calculations. The design optimization is performed for steady-state and full-load condition by using analytical method. To account for transient performance, the objective function is formulated to optimize for PM mass while subjected to the constraints such as output power, back-EMF, start-up torque and air-gap flux density. The rationale behind this is as follows:

- by optimizing the PM material required in the rotor the reactive power exchanged with the power supply will be minimized and a higher power factor can be gained at a lower line current [8]
- however, PM material in the rotor is also responsible for the braking torque during start-up process, which adversely affects the starting performance of a LSPMSM
- thus, a fine balance between the above two is the key for the design of a LSPMSM

All selected rotor topologies are individually optimized to ensure the best candidate designs are found. Once

an optimum design is identified, its start-up and synchronization characteristics will be validated by running a transient time-step FE analysis with the torque-speed curve of a practical fan. In the event that the design does not meet with the start-up or synchronization requirements, new design iterations need to be carried out until a satisfactory design is found. The flow chart of the LSPM motor design procedure is given in Fig. 4.

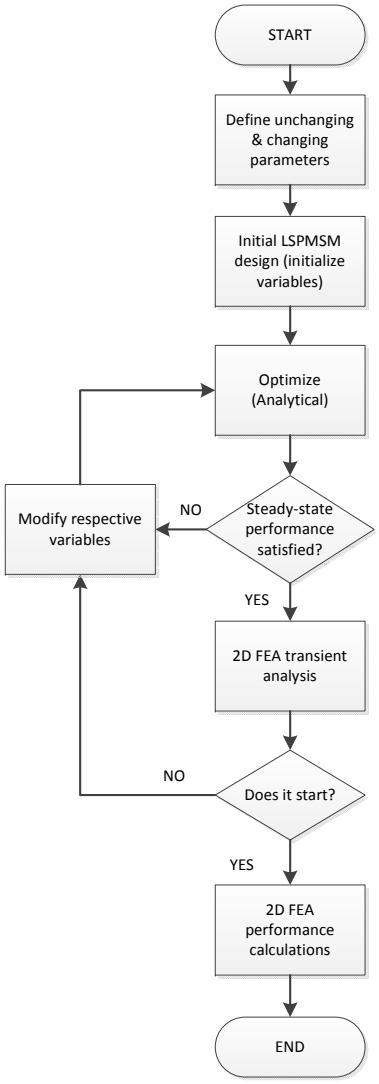

Figure 4: Flow chart of LSPM motor design procedure.

4. PERFORMANCE EVALUATION

In this section the steady-state and transient performance of the four optimized LSPMSMs will be evaluated and compared with each other. The LSPMSM with the best performance is then compared to the reference PEIM.

4.1 Steady-state performance

Table 3 summarizes the steady-state performance of the four optimal LSPMSM designs. It is clear that the second design (D2) shows the best steady-state performance of all. Although it has the highest back-EMF value of the four designs, it has the lowest braking torque component as well. This may be attributed to the higher $d-$ axis inductance that also has a large impact on the braking torque (T_m) represented by the following equation:

$$T_m = \frac{3p}{\omega(1-s)} \left[\frac{R_1^2 + X_q^2(1-s)^2}{R_1^2 + X_q X_d (1-s)^2} \right] \left[\frac{R_1 E_o^2 (1-s)^2}{R_1^2 + X_d X_q (1-s)^2} \right]$$

with p being the pole pairs, ω the electrical angular speed in rad/s, R_1 the stator resistance, X_q and X_d the dq axis inductances, and s the slip at a given instant [9]. Also interesting is that the second design (D2) utilizes the least amount of PM material.

Table 3: Optimized LSPMSMs: steady-state performance.

Description	**D1**	**D2**	**D3**	**D4**
Efficiency, %	95.8	95.98	95.8	95.7
Power factor	0.96	0.97	0.94	0.945
Total loss, W	96	94.2	97.6	98.4
Airgap flux density, T	0.44	0.61	0.48	0.49
Rated current, A	2.63	2.58	2.67	2.67
Braking torque, Nm	16.4	12.5	14.7	13.2
Back EMF, V	346.8	488.7	380.2	387
PM weight, kg	0.78	0.54	0.58	0.6

4.2 Transient performance

The transient performances of LSPMSMs are of particular interest as this type motor is known for its relatively poor transient performance [4]. The transient performance calculations of the four LSPMSM designs are carried out using a transient 2D FE software package. The experimentally determined fan load characteristics are incorporated into the simulation. Fig. 5 shows the flux plot of the Design 2 under full load at a certain time step. The detailed simulation results are included in Appendix A (Figs 6-15).

The transient performance of four designs are compared in Table 4. It is evident that the second design (D2) demonstrates the best transient performance as it reaches synchronization within the shortest time (also refer to Figs 6-9). It can also be seen in Figs 11-14 that the torque-speed trajectory of Design 2 shows less pole-slips repetitions and speed overshoots of all four designs. Better synchronization capability is also evident with a smaller locus around the synchronous speed.

Table 4: Optimized LSPMSMs: transient performance.

Description	D1	D2	D3	D4
Start-up time, s	2	1	1.4	1.25
Start-up current, A	32.5	29	30	32
Start-up torque, Nm	73	72.3	75.4	64

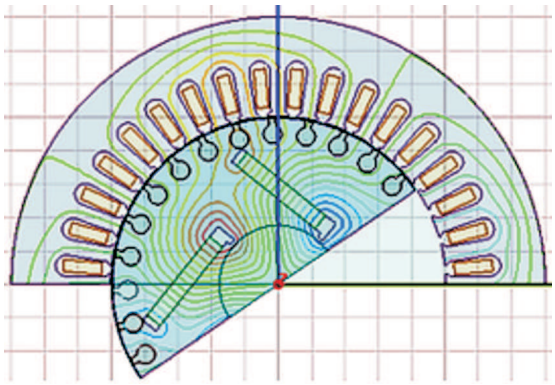

Figure 5: Flux plot of the LSPMSM (design 2) under full load.

4.3 Performance comparison: LSPMSM vs PEIM

Based on the comparison in Sections 4.1 and 4.2, Design 2 can be identified as the best design option of the four designs. The next step is to determine how the performances of Design 2 compare with these of a PEIM under the same load and operation conditions.

From Table 5 it is clear that the Design 2 has a higher efficiency, almost unity power factor, significantly lower steady-state losses and lower rated current. The LSPMSM (D2) also has larger start-up and breakdown torques. The synchronization time between the LSPMSM and PEIM is practically the same. However, the start-up current of LSPMSM is higher than that of PEIM.

Table 5: Performance comparison: LSPMSM vs. PEIM.

Description	LSPMSM (D2)	PEIM
Rated power, kW	2.2	2.2
Rated line current, A	2.61	3.16
Rated speed, RPM	1500	1457
Total loss, W	95	245
Efficiency, %	95.8	90.4
Power factor	0.97	0.88
Air-gap flux density, T	0.59	0.75
Air-gap length, mm	0.5	0.2
Start-up time, s	1	0.9
Start-up current, A	32.5	22.5
Start-up torque, Nm	75.14	51.81
Breakdown torque, Nm	83.95	64.7
Breakdown slip	0.56	0.36

As shown in Figs 12 and 15, for fan-type loads with relatively high inertia, the instantaneous speed-torque trajectory for both LSPM motor and induction motor show signs of repetitive pole-slips profiles at starting. The synchronization process for both motors are satisfactory.

5. CONCLUSION

In this paper, LSPMSMs with different rotor topologies are optimally designed and compared for fan load applications. It clearly shows that Design 2 delivers the best overall performance among the selected designs. Furthermore, the steady-state and transient performances of both Design 2 and the PEIM are computed and compared by applying 2D transient FE analysis. The results show that the LSPMSM (D2) has higher efficiency and power factor compared to the PEIM at steady-state. Although the satisfactory transient starting performance of the LSPMSM is evident, the PEIM draws less starting current and exhibits a slightly better transient performance than the LSPMSM. The transient performance of the LSPMSM might be improved by investigating the cage design in the rotor. From the results provided in this paper it is clear that a LSPMSM can act as a direct replacement for PEIM for fan-load applications.

ACKNOWLEDGMENT

This work was supported in part by Eskom Tertiary Education Support Program (TESP), Sasol Technology Research and Development, and the National Research Foundation (NRF).

REFERENCES

[1] T. Modeer, “Modeling and testing of line start permanent magnet motors,” Master’s thesis, KTH, Stockholm, Sweden, 2007.

[2] I. Boldea, *The induction machine handbook*. New York, USA: CRC Press, 2002.

[3] F. Kalluf, C. Pompermaier, and N. Ferreira da Luz, M.V.and Sadowski, “Braking torque analysis of the single phase line-start permanent magnet synchronous motor,” in *Electrical Machines (ICEM), 2010 XIX International Conference on*, 2010, pp. 1–5.

[4] C. Mutize and R.-J. Wang, “Performanse comparison of an induction machine and line-start PM motor for cooling fan applications,” in *21st Southern African Universities Power Engineering Conference (SAUPEC)*, 2013, pp. 122–126.

[5] W. Kim, K. Kim, K. S.J., D. Kang, S. Go, H. Lee, Y. Chun, and J. Lee, “A study on the optimal rotor design of lspm considering the starting torque and efficiency,” *Magnetics, IEEE Transactions on*, vol. 45, no. 3, pp. 1808–1811, 2009.

[6] P. Hung, S. Mao, M. Tsai, and C. Liu, “Investigation of line start permanent magnet synchronous motors with interior-magnet rotors and surface-magnet rotors,” in *Electrical Machines and Systems (ICEMS), International Conference on*, 2008, pp. 2888–2893.

[7] W. Jazdzynski and M. Bajek, "Modeling and bi-criterial optimization of a line start permanent magnet synchronous machine to find an ie4 class high efficiency motor," in *Electrical Machines (ICEM), 2010 XIX International Conference on*, 2010, pp. 1–5.

[8] D. Rodger, H. Lai, R. Hill-Cottingham, P. Coles, and F. Robinson, "A new high efficiency line start motor with high starting torque," in *Power Electronics, Machines and Drives (PEMD), 2006 IET International Conference*, 2006, pp. 551–555.

[9] V. Honsinger, "Permanent magnet machines: asynchronous operation," *Power Apparatus and Systems, IEEE Transactions on*, vol. 99, no. 4, pp. 1503–1509, 1980.

APPENDIX

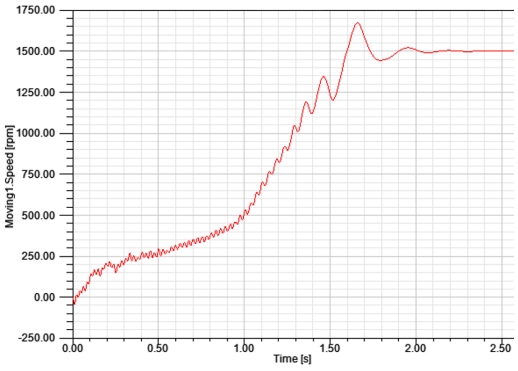

Figure 6: LSPM design 1: speed versus time curves.

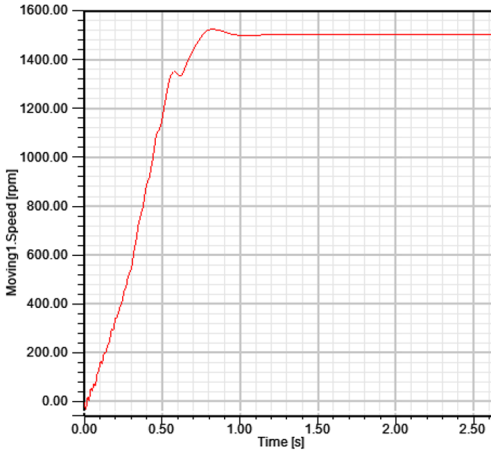

Figure 7: LSPM design 2: speed versus time curves.

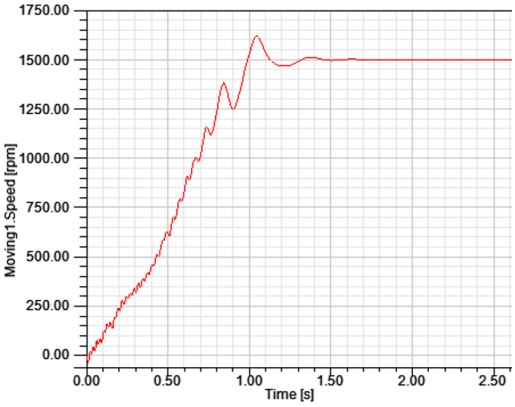

Figure 8: LSPM design 3: speed versus time curves.

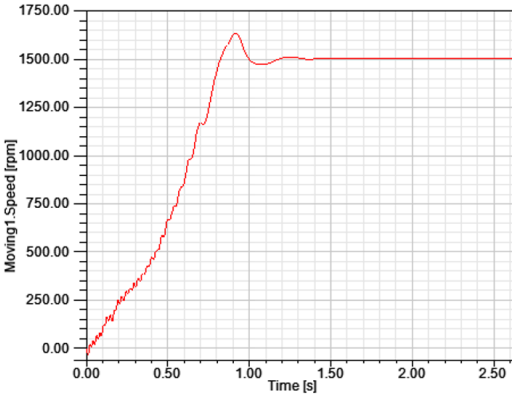

Figure 9: LSPM design 4: speed versus time curves.

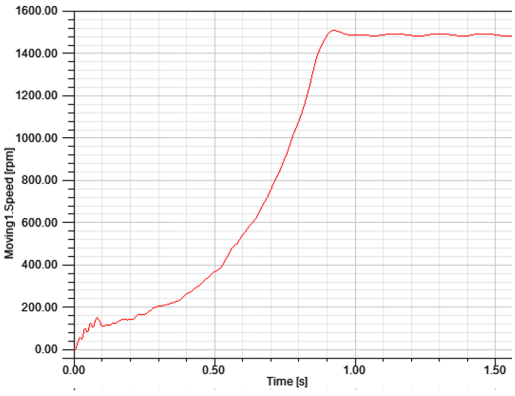

Figure 10: PEIM: speed versus time curves.

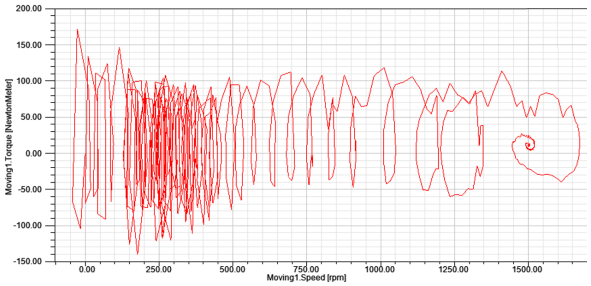

Figure 11: LSPM design 1: transient torque-speed trajectories.

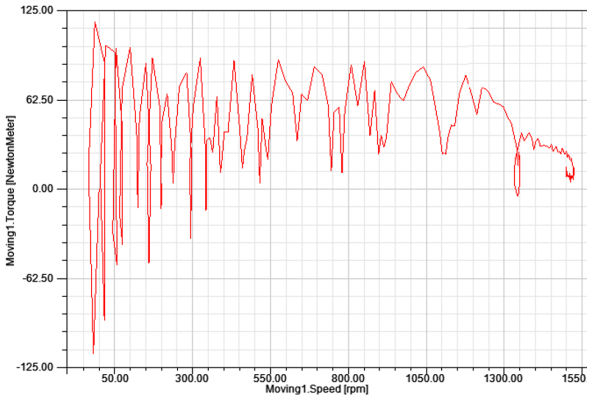

Figure 12: LSPM design 2: transient torque-speed trajectories.

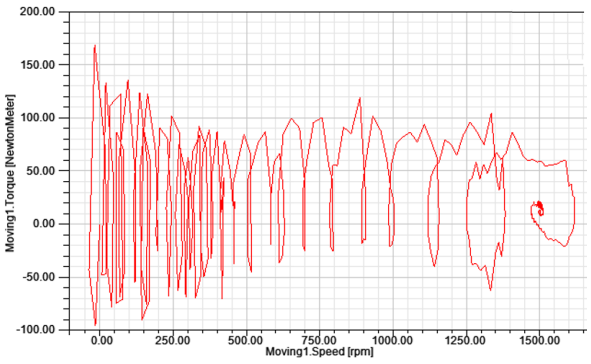

Figure 13: LSPM design 3: transient torque-speed trajectories.

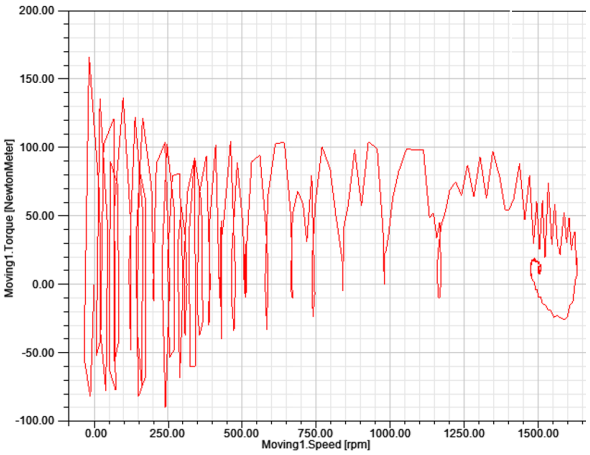

Figure 14: LSPM design 4: transient torque-speed trajectories.

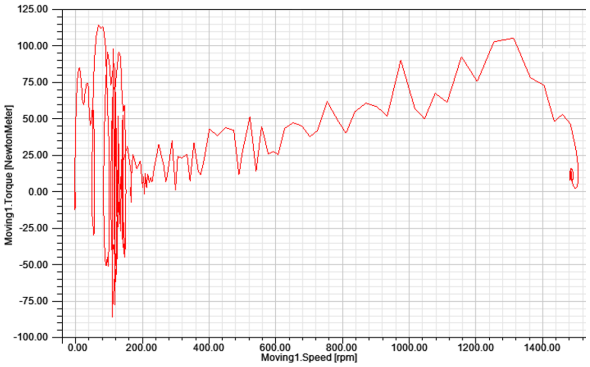

Figure 15: PEIM: transient torque-speed trajectories.